mathematics

MDPI

Article

A Moving-Mesh Finite-Difference Method for Segregated Two-Phase Competition-Diffusion

Michael John Baines † and Katerina Christou *,†

Department of Mathematics and Statistics, School of Mathematical, Physical and Computational Sciences (SMPCS), Faculty of Science, University of Reading, Reading RG6 6AH, UK; m.j.baines@reading.ac.uk

* Correspondence: k.christou@pgr.reading.ac.uk

† These authors contributed equally to this work.

Abstract: A moving-mesh finite-difference solution of a Lotka-Volterra competition-diffusion model of theoretical ecology is described in which the competition is sufficiently strong to spatially segregate the two populations, leading to a two-phase problem with a coupling condition at the moving interface. A moving mesh approach preserves the identities of the two species in space and time, so that the parameters always refer to the correct population. The model is implemented numerically with a variety of parameter combinations, illustrating how the populations may evolve in time.

Keywords: segregation; competition; interface condition; velocity-based moving meshes; finite-differences

Citation: Baines, M.J.; Christou, K. A Moving-Mesh Finite-Difference Method for Segregated Two-Phase Competition-Diffusion. *Mathematics* **2021**, *9*, 386. https://doi.org/10.3390/math9040386

Academic Editor: Yuri Luchko

Received: 27 December 2020

Accepted: 8 February 2021

Published: 15 February 2021

1. Introduction

Ecological competition is a widely studied concept in both theoretical and experimental ecology. In particular, the interspecific competition has long been one of ecology's most prevailing pursuits as it is one of the factors that affect the evolution of species and can alter populations and community structure.

Many researchers have made efforts to develop models to investigate species competition from the viewpoint of mathematical ecology. For a theoretical understanding of spatial patterns arising in population dynamics for competitive species, several free boundary problems have been proposed [1–5] which provide useful theoretical results. Various numerical methods have been applied to solve such free boundary problems, for instance, in [6] the authors use a front tracking approach and a front fixing approach to a two-species competition-diffusion model with two free boundaries, whereas in [7] a moving mesh finite element method is used solve a two competitive segregated species that cannot coexist in space.

Due to the complexity of the equations numerical approximation is useful both for extracting quantitative solutions and for achieving a qualitative understanding of the behaviour of the solution. However, special attention must be paid to the moving interface, whose location usually requires higher resolution than the rest of the domain while the solution may exhibit singular behaviour there.

To avoid this difficulty adaptive methods have been used which modify the resolution of the domain as the solution evolves in response to changes in the dependent variable. Adaptive methods become preferable to fixed mesh methods when the areas of interest are a fraction of the domain, such as the moving interface. With adaptive methods greater precision can be achieved locally without having to increase the resolution everywhere in the domain, which would lead to a very computationally expensive scheme.

There are three most used adaptive mesh methods, namely *h*-, *p*-, and *r*-refinement. The first involves repeated subdivision of intervals of a fixed mesh around the areas of interest. The second is often used in combination with *h*-refinement and includes higher-order polynomials in each interval between the mesh points, so that functions are better

approximated. Finally, *r*-refinement is the movement of existing mesh points at each time-step to track a feature of interest.

Constructions of *r*-refinement moving mesh methods vary considerably. In [8] moving mesh methods are classified as velocity-based or location-based approaches. In the latter case the solution is found from a moving form of the PDE which is solved simultaneously with a mesh equation to generate the node position and the solution together. This moving mesh approach (MMPDE) is described in [9,10], see also the Moving Finite Element method [11,12]. In the present paper a velocity-based *r*-refinement scheme is used in which the mesh is generated by one Eulerian conservation principle while the solution is determined algebraically from a Lagrangian form of conservation [13–15]. We first briefly describe the moving mesh method based on conservation.

The conservation method uses an integral to preserve a desired conserved quantity within each patch of elements from which the velocities are constructed. For a mass conserving problem, in which the global mass is constant this quantity is the conserved local mass. However, for a non-mass conserving problem the theory uses the concept of relative mass. By the Leibniz Integral Rule we can then construct an equation from which the velocity of each node is derived. For a unique solution of that equation, the population density must be known at a node or a velocity must be applied to a node which may be thought of as an 'anchor' point.

The approach used in this paper is similar to the finite difference method used in [15] where the method was applied to one-dimensional moving boundary problems such as the mass conserving porous medium equation, Richard equation in hydrology, and the Crank-Gupta problem that does not conserve mass. Finite element versions of the velocity-based moving mesh approach have been used by Baines, Hubbard and Jimack in [13,14] and by Baines, Hubbard, Jimack and Mahmood in [16].

In this paper we apply the moving mesh finite difference method based on conservation to a PDE system of Lotka-Volterra competition model, first proposed by [17], which describes a two phase segregated reaction-diffusion system with a high competition limit where the species are completely spatially segregated and only interact through an interface condition. It is shown in [17] that where the competition is strong enough to spatially segregate the two populations the Lotka-Volterra system can be reduced to a form similar to a Stefan problem in physics [18]. The two major differences are firstly, that there are additional logistic growth terms in the Lotka-Volterra model and secondly, there is a parameter in the Lotka-Volterra model of the interface condition (the equivalent of the latent heat coefficient of the Stefan problem) which is set equal to zero. Unlike the Stefan problem, one species does not transform into another which means that the competition system has an interface condition that specifies the interface velocity only implicitly.

In [19] the authors considered the segregation problem due to high competition with inhomogeneous Dirichlet boundary condition while similar studies in the case of Neumann boundary conditions are presented in [20,21].

The system of equations presented in this paper is suitable to describe concepts in ecology when two species with similar ecological niches cannot co-exist, known as the competitive exclusion principle [22]. One will always overcome the other, so the more competitive species will stay and the subordinate one will either adapt or be excluded by either emigration or extinction.

The layout of the paper is as follows. Section 2 gives details of the Lotka-Volterra competition model with a high competitive rate and describes the relative conservation principle approach and its finite difference implementation, together with the algorithm of the moving mesh finite difference method. In Section 3 illustrations are given for a variety of parameter combinations, observing the various behaviours that dominate as the species evolve through time. Finally, Section 4 gives a brief discussion of the results and potential research directions.

2. Materials and Methods

2.1. The Lotka-Volterra System

The Lotka-Volterra system is the two-component reaction-diffusion system

$$\frac{\partial u_1}{\partial t} = \delta_1 \frac{\partial^2 u_1}{\partial x^2} + f(u_1, u_2)u_1 \qquad x \in R_1(t), \quad t > 0 \tag{1}$$

$$\frac{\partial u_2}{\partial t} = \delta_2 \frac{\partial^2 u_2}{\partial x^2} + g(u_1, u_2)u_2 \qquad x \in R_2(t) \quad t > 0 \tag{2}$$

where $u_1(x,t)$ and $u_2(x,t)$ are the population densities of two competing species in abutting regions $R_1(t)$ and $R_2(t)$, the parameters δ_1, δ_2 are constant diffusion coefficients, and

$$f(u_1, u_2) = r_1\left(1 - \frac{u_1 + K_1 u_2}{k_1}\right)$$

$$g(u_1, u_2) = r_2\left(1 - \frac{u_2 + K_2 u_1}{k_2}\right).$$

are reaction terms in which K_1, K_2 are species-specific competition rates, k_1, k_2 are the carrying capacities of the species, and $r_1, r_2 > 0$ are reproductive rate parameters.

In [17] it is demonstrated that for two species completely segregated the reaction terms can be reduced to

$$f(u_1, u_2) = r_1(1 - u_1/k_1)$$

$$g(u_1, u_2) = r_2(1 - u_2/k_2).$$

so that Equations (1) and (2) become

$$\frac{\partial u_1}{\partial t} = \delta_1 \frac{\partial^2 u_1}{\partial x^2} + \left\{r_1\left(1 - \frac{u_1}{k_1}\right)\right\}u_1 \qquad x \in R_1(t), \quad t > 0 \tag{3}$$

$$\frac{\partial u_2}{\partial t} = \delta_2 \frac{\partial^2 u_2}{\partial x^2} + \left\{r_2\left(1 - \frac{u_2}{k_2}\right)\right\}u_2 \qquad x \in R_2(t) \quad t > 0 \tag{4}$$

The resulting system represents the limit in which the carrying capacities k_1, k_2 values are very large, i.e., the competition rate is high enough that the two species cannot coexist in space and interact only through the interface boundary.

Initial conditions on u_1 and u_2 are selected such that one species is in growth and the other in decline. These are shown in Figure 1.

Zero Neumann boundary conditions $\partial u_1/\partial x = 0$ and $\partial u_2/\partial x = 0$ are applied at fixed external boundaries away from the interface.

2.2. The Interface Conditions

At the interface between the two species there is a condition that gives the relationship between their fluxes. In essence, the species both flow into the interface and annihilate each other with a rate determined by the ratio of the interspecific competition coefficients $\mu = \frac{K_2}{K_1}$. This condition is given as

$$\mu\delta_1 \frac{\partial u_1}{\partial x} = -\delta_2 \frac{\partial u_2}{\partial x}. \tag{5}$$

Because the annihilation is complete we also have zero Dirichlet conditions $u_1 = u_2 = 0$ at the interface.

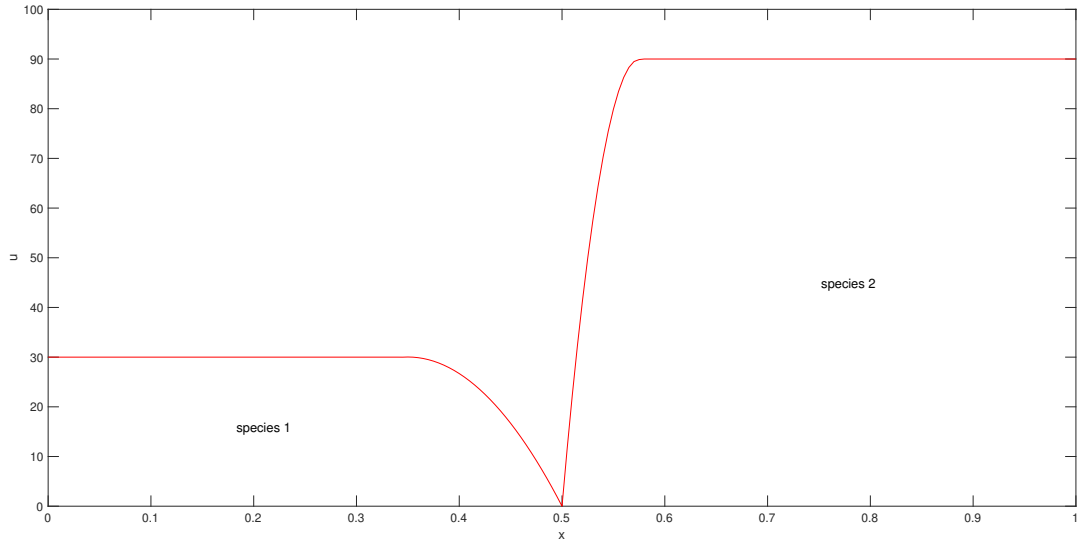

Figure 1. Initial conditions for the competition system, with population density u_1 of species 1 and u_2 of species 2 presented by the graph in $0 \leq x \leq 0.5$ and in $0.5 \leq x \leq 1$ respectively. The interface node has zero population and must always satisfy the interface condition.

2.3. The MMFDM Conservation Method

2.3.1. A Relative Conservation Principle

Define the total population of species p as

$$\theta_p(t) = \int_{R_p(t)} u_p(x,t)\,\mathrm{d}x$$

$(p = 1, 2)$. Then by Leibnitz' Integral Rule,

$$\dot{\theta}_p = \frac{\mathrm{d}\theta_p}{\mathrm{d}t} = \frac{\mathrm{d}}{\mathrm{d}t}\int_{R_p(t)} u_p(x,t)\,\mathrm{d}x = \int_{R_p(t)} \frac{\partial u_p}{\partial t}\,\mathrm{d}x + \left[u_p v_p\right]_{R_p(t)}$$

The final term vanishes by the boundary and interface conditions, so

$$\dot{\theta}_p = \int_{R_p(t)} \frac{\partial u_p}{\partial t}\,\mathrm{d}x \qquad (p = 1, 2).$$

From (3) and (4),

$$\dot{\theta}_p = \int_{R_p(t)} \left(\delta_p \frac{\partial^2 u_p}{\partial x^2} + \left\{ r_p \left(1 - \frac{u_p}{k_p} \right) \right\} u_p \right) \mathrm{d}x \qquad (p = 1, 2) \tag{6}$$

which can be integrated in time to give θ_p.

We now suppose that population *fractions* $c(\Omega_p)$

$$c(\Omega_p) = \frac{1}{\theta_p(t)} \int_{\Omega_p(t)} u_p(x,t)\,\mathrm{d}x, \qquad (p = 1, 2), \tag{7}$$

in each moving subdomain $\Omega_p(t)$ are independent of time, so that $\theta_p(t)$ and $u_p(x,t)$ satisfy the *relative* conservation principle

$$c(\Omega_p) = \int_{\Omega_p(t)} \frac{1}{\theta_p(t)} u_p(x,t)\,\mathrm{d}x, \qquad (p = 1, 2), \tag{8}$$

Note that $\frac{u_p}{\theta_p}$ are conserved quantities.

Since the population fractions $c(\Omega_p)$ are constant in time, they are determined by the conditions at the initial time t^0, i.e.,

$$c(\Omega_p) = \frac{1}{\theta_p(t^0)} \int_{R_p(t^0)} u_p(x, t^0)\, \mathrm{d}x$$

Writing (8) as

$$\int_{\Omega_p(t)} u_p(x,t)\, \mathrm{d}x = c(\Omega_p)\theta_p(t), \qquad (p = 1,2). \tag{9}$$

and differentiating the left hand side of (9) with respect to time using Leibnitz Integral Rule,

$$\frac{\mathrm{d}}{\mathrm{d}t}\left[\int_{\Omega_p(t)} u_p(x,t)\mathrm{d}x\right] = \int_{\Omega_p(t)} \left(\frac{\partial u_p}{\partial t} + \frac{\partial}{\partial x}(u_p v_p)\right)\mathrm{d}x, \qquad (p = 1,2)$$

where v_p is the velocity of points of the domain. Therefore, by (9), given the population fractions $c(\Omega_p)$ of the total mass $\dot{\theta}_p$, the velocity v_p and u_p satisfy the equations

$$c(\Omega_p)\dot{\theta}_p - \int_{\Omega_p(t)} \frac{\partial}{\partial x}(u_p v_p)\mathrm{d}x = \int_{\Omega_p(t)} \frac{\partial u_p}{\partial t}\mathrm{d}x, \qquad (p = 1,2),$$

where the $\dot{\theta}_p$ are given by (3) or (4), leading to

$$c(\Omega_p)\dot{\theta_p} - \left[u_p v_p\right]_{\Omega_p(t)} = \delta_p \left[\frac{\partial u_p}{\partial x}\right]_{\Omega_p(t)} + r_p \int_{\Omega_p(t)} u_p(x,t)\left(1 - \frac{u_p(x,t)}{k_p}\right)\mathrm{d}x, \tag{10}$$

We let the subdomains $\Omega_1(t)$ in the region $R_1(t)$ consist of the interval $(a, x(t))$ where a is a fixed boundary and let $x(t)$ be any point in the region $R_1(t)$. Similarly the subdomains $\Omega_2(t)$ in the region $R_2(t)$ consist of the interval $(x(t), b)$ where b is a fixed boundary and $x(t)$ is any point in the region $R_2(t)$.

The boundary conditions at the external boundaries a and b are $\partial u_1/\partial x = \partial u_2/\partial x = 0$, and also $v_1 = v_2 = 0$ because the boundaries are fixed. Together with the condition that $u_1 = u_2 = 0$ at the interface boundary, Equation (10) for the velocities v_1 and v_2 and the rates of change of the total mass $\dot{\theta}_1$ and $\dot{\theta}_2$ satisfy

$$c_1(x)\dot{\theta_1} - (u_1 v_1)|_{x(t)} = \delta_1 \left.\frac{\partial u_1}{\partial x}\right|_{x(t)} + r_1 \int_a^{x(t)} u_1(x,t)\left(1 - \frac{u_1(x,t)}{k_1}\right)\mathrm{d}x \tag{11}$$

and

$$c_2(x)\dot{\theta_2} + (u_2 v_2)|_{x(t)} = -\delta_2 \left.\frac{\partial u_2}{\partial x}\right|_{x(t)} + r_2 \int_{x(t)}^b u_2(x,t)\left(1 - \frac{u_2(x,t)}{k_2}\right)\mathrm{d}x \tag{12}$$

respectively, where

$$\theta_1 = \int_0^{x_m(t)} u(x,t)\, \mathrm{d}x, \qquad \theta_2 = \int_{x_m(t)}^1 u(x,t)\, \mathrm{d}x$$

and

$$c_1(x) = \frac{1}{\theta_1(t)} \int_0^{x(t)} u(x,t)\, \mathrm{d}x, \qquad c_2(x) = \frac{1}{\theta_2(t)} \int_{x(t)}^1 u(x,t)\, \mathrm{d}x$$

From (6),

$$\dot{\theta_1} = \delta_1 \left.\frac{\partial u_1}{\partial x}\right|_{x_m(t)} + r_1 \int_a^{x_m(t)} u_1(x,t)\left(1 - \frac{u_1(x,t)}{k_1}\right)\mathrm{d}x \tag{13}$$

and

$$\dot{\theta_2} = -\delta_2 \left.\frac{\partial u_2}{\partial x}\right|_{x_m(t)} + r_2 \int_{x_m(t)}^{b} u_2(x,t)\left(1 - \frac{u_2(x,t)}{k_2}\right)\mathrm{d}x \tag{14}$$

2.3.2. The Interface Condition

Since the population density $u = 0$ at the interface and the population densities either side of the interface are positive, the density function is 'V' shaped at the interface.

From [17] the interface condition is given by (5). Whilst the interface velocity is not given explicitly by (5) this equation does determine the location of the interface implicitly. Thus, if we know $\partial u/\partial x$ adjacent to the interface in each region we may use the condition that $u = 0$ at the interface to infer an interface position such that the values of $\delta_p \partial u_p/\partial x$ either side of the interface are in the ratio $-\mu$.

We now describe a finite difference numerical method for the solution of the problem.

2.3.3. Numerical Solution

Let the domain (a, b) be $(0, 1)$. At time level $t = t^n$ define time-dependent mesh points

$$0 = x_0 < x_1^n < \ldots < x_{m-1}^n < x_m^n < x_{m+1}^n < \ldots < x_N^n < x_{N+1}^n = 1$$

where x_m^n is the node at the moving interface, and let u_i^n, $(0 \le i \le N+1)$, approximate $u(x,t)$ by u_i^n at these points.

The initial values θ_1^0 and θ_2^0 of the total mass approximations $\theta_1^n \approx \theta_1(t)$ and $\theta_2^n \approx \theta_2(t)$ of (13) and (14) are estimated by the composite trapezium rule

$$\theta_1^0 = \sum_{i=1}^{m} \frac{1}{2}(u_{i-1}^0 + u_i^0)(x_i^0 - x_{i-1}^0), \qquad \theta_2^0 = \sum_{i=m}^{N} \frac{1}{2}(u_i^0 + u_{i+1}^0)(x_{i+1}^0 - x_i^0), \tag{15}$$

and the constant-in-time relative masses $c_{1,i}$ and $c_{2,i}$ in the interval (x_{i-1}^n, x_i^n) by

$$c_{1,i} = \frac{1}{\theta_1^0}\frac{1}{2}(u_i^0 + u_{i+1}^0)(x_{i+1}^0 - x_i^0), \qquad (0 \le i < m-1), \tag{16}$$

$$c_{2,i} = \frac{1}{\theta_2^0}\frac{1}{2}(u_i^0 + u_{i-1}^0)(x_i^0 - x_{i-1}^0), \qquad (m+1 < i \le N+1), \tag{17}$$

at the initial time $t = t^0$.

For the initial conditions we take the x_i^0 to be equally spaced and the u_i^0 pointwise from an initial function

$$\begin{aligned}
&u(x,0) = 30, && (0 \le x \le 0.34)\\
&u(x,0) = (x-0.2)(0.5-x) \times 170 \times 7.85, && (0.35 \le x \le 0.5)\\
&u(x,0) = 0, && (x = 0.51)\\
&u(x,0) = (x-0.65)(0.5-x) \times 170 \times 94, && (0.52 \le x \le 0.58)\\
&u(x,0) = 90, && (0.59 \le x \le 1)
\end{aligned}$$

chosen to resemble the one in [7] (see Figure 1).

We remark that in the case of the chosen initial conditions, a uniform mesh x_i^0 can be obtained only for an odd N.

2.3.4. Rates of Change of the Total Populations

The rates of change of the total populations $\dot{\theta}_1, \dot{\theta}_2$ of (6) are approximated by composite trapezium rules, in region 1 from (13),

$$\dot{\theta}_1^n = \delta_1 \left(\frac{u_m^n - u_{m-1}^n}{x_m^n - x_{m-1}^n}\right)$$

$$+r_1 \sum_{i=1}^{m} \frac{1}{2}\left\{ u_{i-1}^n \left(1 - \frac{u_{i-1}^n}{k_1}\right) + u_i^n \left(1 - \frac{u_i^n}{k_1}\right)\right\}(x_i^n - x_{i-1}^n) \tag{18}$$

and in region 2, from (14),

$$\dot{\theta}_2^n = -\delta_2 \left(\frac{u_{m+1}^n - u_m^n}{x_{m+1}^n - x_m^n} \right)$$

$$+r_2 \sum_{i=m}^{N} \frac{1}{2}\left\{ u_i^n \left(1 - \frac{u_i^n}{k_2}\right) + u_{i+1}^n \left(1 - \frac{u_{i+1}^n}{k_2}\right)\right\}(x_{i+1}^n - x_i^n) \tag{19}$$

2.3.5. Approximating the Velocities

From (11), using the composite trapezium rule, the velocity v_i^n in region 1 satisfies,

$$c_{1,i}\dot{\theta}_1^n + u_i^n v_i^n = \delta_1 \left.\frac{\partial u}{\partial x}\right|_m^i$$

$$+r_1 \sum_{j=2}^{i} \frac{1}{2}\left\{ u_{j-1}^n \left(1 - \frac{u_{j-1}^n}{k_1}\right) + u_j^n \left(1 - \frac{u_j^n}{k_1}\right)\right\}(x_j^n - x_{j-1}^n), \quad (1 < i < m-1),$$

where we have taken the subdomain Ω_1^n to be the interval (x^n, x_m^n). Similarly, from (12), the velocity v_2^n in region 2 satisfies

$$c_{2,i}\dot{\theta}_2^n + u_i^n v_i^n = -\delta_2 \left.\frac{\partial u}{\partial x}\right|_m^i$$

$$+r_2 \sum_{j=i}^{N} \frac{1}{2}\left\{ u_j^n \left(1 - \frac{u_j^n}{k_2}\right) + u_{j+1}^n \left(1 - \frac{u_{j+1}^n}{k_2}\right)\right\}(x_{j+1}^n - x_j^n), \quad (m+1 < i < N).$$

where we have taken the subdomain Ω_2^n to be the interval (x_m^n, x^n).

2.3.6. Time-Stepping

For the time integration we adopt an explicit Euler time-stepping approach. Given the u_i, we update the total masses θ_p from the equation $\dot{\theta}_p = \mathrm{d}\theta_p/\mathrm{d}t$, $(p = 1, 2)$ using (18) and (19) by

$$\theta_p^{n+1} = \theta_p^n + \Delta t\, \dot{\theta}_p^n \tag{20}$$

$(p = 1, 2)$, where Δt is the time step, and the mesh points x_i^n are updated from the equation $\mathrm{d}x_i/\mathrm{d}t = v_i$ by

$$x_i^{n+1} = x_i^n + \Delta t\, v_i^n \qquad (i \neq m), \tag{21}$$

The updates are first-order accurate in time and subject to limitations on the time step to preserve node ordering.

The explicit Euler method is adequate since the time step used is small and the main purpose of the paper is the treatment of the interface. Implicit schemes for the nonlinear Equations (3) and (4) require convergence of an iteration, details of which are not central to the method. Higher order explicit schemes can be found in [23,24].

Note that in case of a zero velocity there is the following well-known sufficient condition on a time step Δt in the explicit scheme to prevent the u_i^{n+1} (and hence the local mass in an interval) going unstable,

$$\frac{\delta_p \Delta t}{(\Delta x_{min})^2} \leq \frac{1}{2}, \quad (p = 1, 2) \tag{22}$$

Here we take (22) as a guide for a safe time step in the moving mesh case.

2.3.7. The Population Densities

In order to determine the approximate population densities u_i at the new time step $t = t^{n+1}$ from the θ_p^{n+1} and x_i^{n+1} we approximate the relative conservation principle (8) as

$$\frac{1}{\theta_p^{n+1}}(x_{i+1}^{n+1} - x_{i-1}^{n+1})u_i^{n+1} = \bar{c}_{p,i} \qquad (p = 1, 2), \tag{23}$$

where from (16) and (17) the constants

$$\bar{c}_{p,i} = \frac{1}{\theta_p^0}(x_{i+1}^0 - x_{i-1}^0)u_i^0 \qquad (p = 1, 2), \tag{24}$$

are dependent only on initial values.

Thus, once the x_i^{n+1} have been found, in region 1, the approximate population density u_i^{n+1} is given by

$$u_i^{n+1} = \frac{\bar{c}_{1,i}\theta_1^{n+1}}{(x_{i+1}^{n+1} - x_i^{n+1})}, \qquad (0 \le i \le m-1), \tag{25}$$

and in that region 2 by

$$u_i^{n+1} = \frac{\bar{c}_{2,i}\theta_2^{n+1}}{(x_i^{n+1} - x_{i-1}^{n+1})} \qquad (m+1 \le i \le N+1). \tag{26}$$

while $u_m^{n+1} = 0$ from the interface condition.

Note that the values of $u_{m\pm1}^{n+1}$ determined by (23) depend on x_m^{n+1}, which is not yet known at t^{n+1}. This value can however be found using the one-sided approximations

$$u_{m-1}^{n+1} = \frac{c_1\theta_1^{n+1}}{\frac{1}{2}(x_{m-1}^{n+1} - x_{m-2}^{n+1})}, \qquad u_{m+1}^{n+1} = \frac{c_2\theta_2^{n+1}}{\frac{1}{2}(x_{m+2}^{n+1} - x_{m+1}^{n+1})}$$

where from (16) and (17)

$$c_1 = \frac{1}{2}u_{m-1}^0(x_{m-1}^0 - x_{m-2}^0), \quad c_2 = \frac{1}{2}u_{m+1}^0(x_{m+2}^0 - x_{m+1}^0)$$

2.3.8. Approximating the Interface

The interface condition (5) is approximated by

$$\mu\delta_1\frac{u_m - u_{m-1}}{x_m - x_{m-1}} = -\delta_2\frac{u_{m+1} - u_m}{x_{m+1} - x_m}, \tag{27}$$

where the subscript m denotes the interface node and the $x_{m\pm1}, u_{m\pm1}$ are adjacent node positions and solution values. Since $u_m = 0$, from (27) an approximation to the position of the interface node x_m^{n+1} in terms of adjacent nodal values at $m \pm 1$ is

$$x_m^{n+1} = \left(\frac{\mu\delta_1 u_{m-1}^{n+1}x_{m+1}^{n+1} + \delta_2 u_{m+1}^{n+1}x_{m-1}^{n+1}}{\mu\delta_1 u_{m-1}^{n+1} + \delta_2 u_{m+1}^{n+1}}\right). \tag{28}$$

Thus, once the other x_i^{n+1}, u_i^{n+1} have been updated, x_m^{n+1} can be found from (28).

2.4. Algorithm

In summary, the moving mesh finite difference solution of the competition-diffusion problem given by Equations (3) and (4) with the interface condition (5) on the moving mesh in 1-D generated by (8) is given by the following algorithm.

From the initial mesh and the initial condition compute the initial values $\theta_p(0)$, $(p = 1, 2)$ of the total populations of the species from (15) and the values of the relative masses $c_{p,i}$ and $\bar{c}_{p,i}$ from (16), (17) and (24).

Then for each time step:

1. Find the rates of change $\dot{\theta}_1, \dot{\theta}_2$ of the total masses from (18) and (19),
2. Calculate the nodal velocities v_i from (11) and (12),
3. Update θ_1 and θ_2 from $\dot{\theta}_1$ and $\dot{\theta}_2$ using the explicit Euler scheme (20),
4. Generate the nodes x_i at the next time-step from the v_i using the explicit Euler scheme (21),
5. Update the population densities u_i at the next time level in each region from (25) and (26),
6. Update the new position of the interface node x_m at the next time level from (28).

3. Results

We find that the model is stable and robust for a variety of parameter choices even when using the explicit Euler integration scheme when using a sufficiently small time step. We observe minimal oscillations affecting the smoothness of the results.

3.1. A Parameter Choice

In the body of work concerning Lotka-Volterra equations there is a vast range of parameter values in use because there are so many varied but suitable examples of the type of competition that are described here. We select a conservatively representative set of parameters, chosen to demonstrate some of the behaviour that this model is able to describe.

For the first example we choose a set of parameters that favour species 1, namely $\delta_1 = \delta_2 = 0.01$, $k_1 = k_2 = 100$, $r_1 = r_2 = 1$ and $\mu = 3$. Even if species 2 makes territorial gains at early stages with the moving interface shifting towards left, the increase in mass of species 1 becomes its weapon to transform it from the inferior species to the superior one (Figure 2). The moving interface changes direction, moving towards the right at an approximately constant velocity where species 1 continues to increase in density with a rate that decreases as time progresses (Figure 3). As we approach the annihilation of species 2, the interface velocity increases again. This is due to the low mass of species 2 affecting its ability to grow (Figure 4). The movement of the interface is shown in Figure 5.

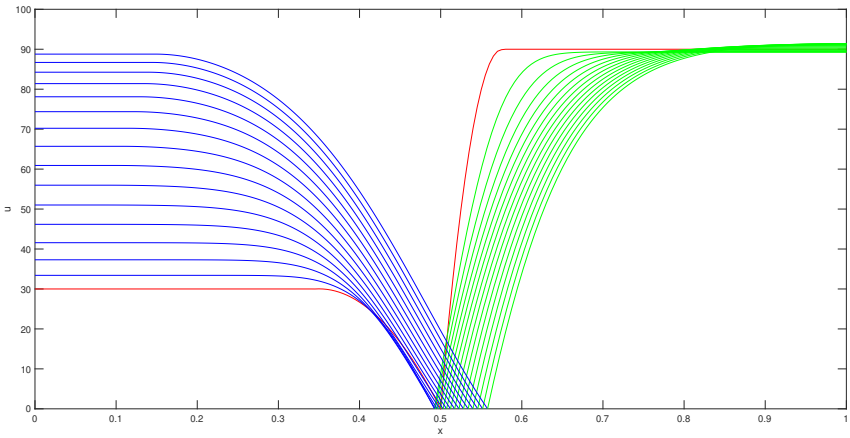

Figure 2. Result of competition model at $t = 1.5$. Here we use $\delta_1 = \delta_2 = 0.01$, $k_1 = k_2 = 100$, $r_1 = r_2 = 1$ and $\mu = 3$. We run the model with a time step of 0.00001 for 150,000 iterations and plot the results every 0.01.We see the internal dynamics of the species driving the population densities and interface fluxes, and the position of the interface responding to those fluxes. The initial conditions are shown in red, with species 1 in blue and species 2 in green.

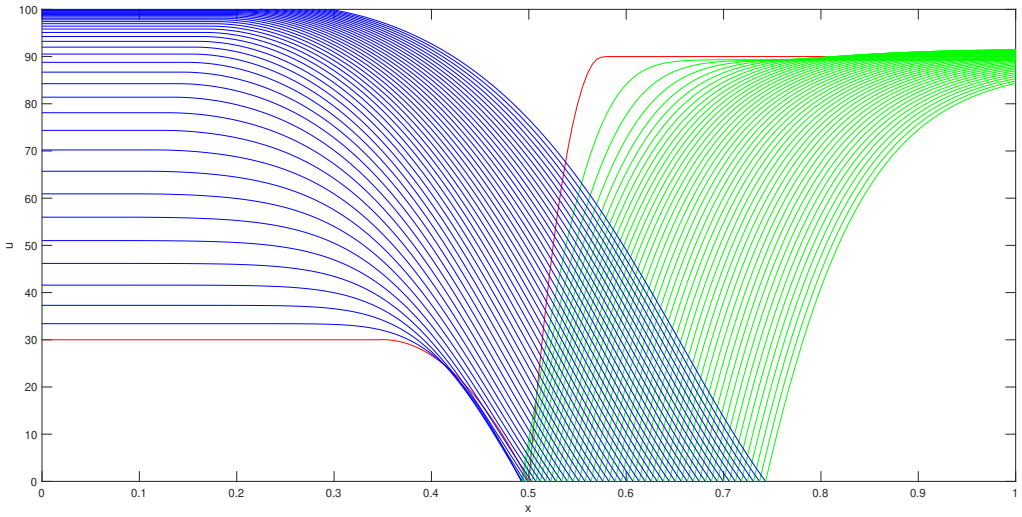

Figure 3. Result of competition model at $t = 4.5$. Here we use $\delta_1 = \delta_2 = 0.01$, $k_1 = k_2 = 100$, $r_1 = r_2 = 1$ and $\mu = 3$. We run the model with a time step of 0.00001 for 450,000 iterations and plot the results every 0.01. The interface continues to evolve and the masses of the species are now limited by the respective carrying capacities. The initial conditions are shown in red, with species 1 in blue and species 2 in green.

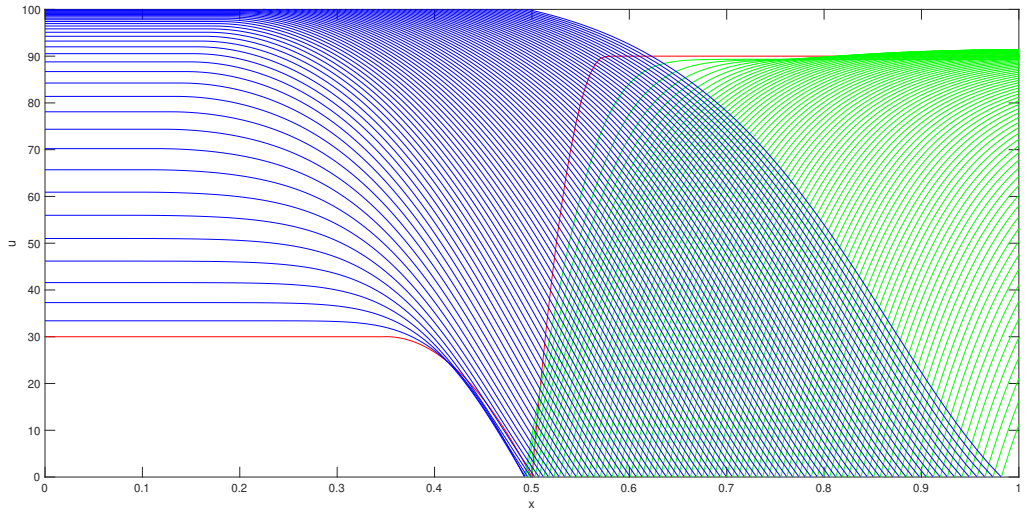

Figure 4. Result of competition model at $t = 8$. Here we use $\delta_1 = \delta_2 = 0.01$, $k_1 = k_2 = 100$, $r_1 = r_2 = 1$ and $\mu = 3$. We run the model with a time step of 0.00001 for 800,000 iterations and plot the results every 0.01. We observe that whilst species 2 initially grew in mass, it will now be wiped out by competition with species 1.The initial conditions are shown in red, with species 1 in blue and species 2 in green.

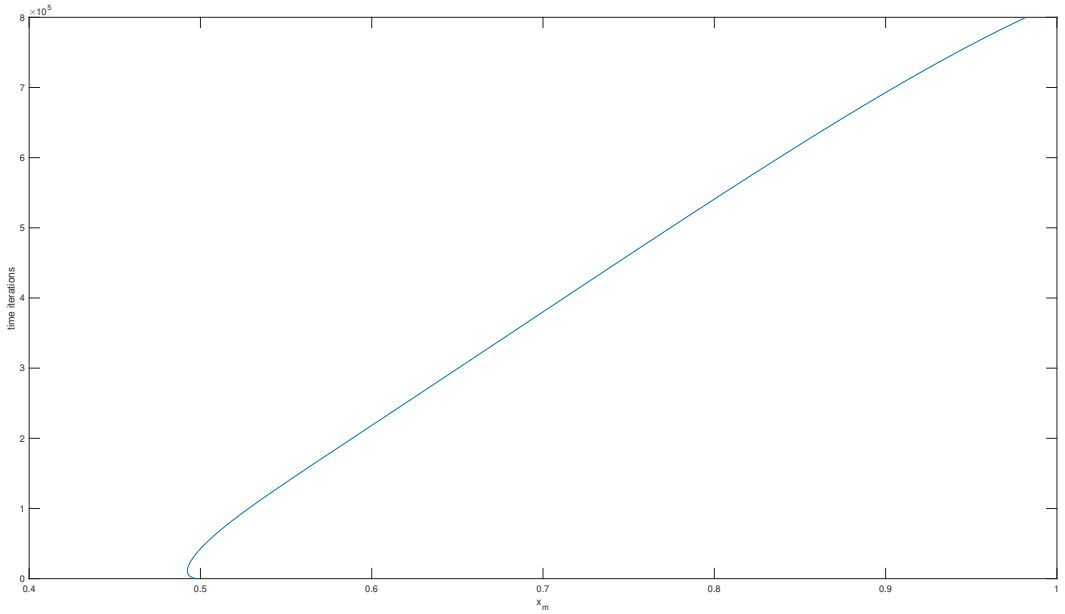

Figure 5. Movement of the interface position x_m for the competition model with parameters $\delta_1 = \delta_2 = 0.01$, $k_1 = k_2 = 100$, $r_1 = r_2 = 1$ and $\mu = 3$. We run the model with a time step of 0.00001 for 800,000 iterations. We see the interface velocity accelerate as we approach an annihilation event.

3.2. Other Parameter Choices

3.2.1. Carrying Capacities

We now investigate other parameter choices. We restrict the growth of species 1 by lowering its carrying capacity and observe that in this scenario neither species is dominant, even though all the competition and diffusion characteristics are unchanged. Here we use $\delta_1 = \delta_2 = 0.01$, $k_1 = 50, k_2 = 150$, $r_1 = r_2 = 1$ and $\mu = 3$. With these differently chosen carrying capacities we find that the interface position is approximately steady and the two species are in balance. This scenario is shown in Figure 6. Density dependence can affect the ability of a species to compete. In the case of decreasing the carrying capacity of species 1 we observe that species can both exist in space, still competing for common resources with none shifting towards other regions in space or in some cases becoming extinct.

3.2.2. Diffusion Characteristics

Alternatively we may adjust the diffusion characteristics of the system. By allowing species 2 to diffuse at a higher rate, we observe that species 2 is able to make territorial gains due to this property alone (Figure 7). Here we use $\delta_1 = 0.01, \delta_2 = 0.05$, $k_1 = k_2 = 100$, $r_1 = r_2 = 1$ and $\mu = 3$. Due to the growth characteristics, we can see interesting temporal effects. Here the interface velocity has actually reversed directions as the system changes from diffusion dominated to growth dominated. We observe that species 2 is able to make territory gains initially due to its high diffusion rate, even though the competition rate is unaltered. However, as time goes on, the growth and competition characteristics become increasingly important. We see species 1 becoming more dominant over time, so that the interface velocity actually reverses direction.

Figure 8 shows the evolution of the system at $t = 11$ and Figure 9 shows the movement of the interface with the direction reversal.

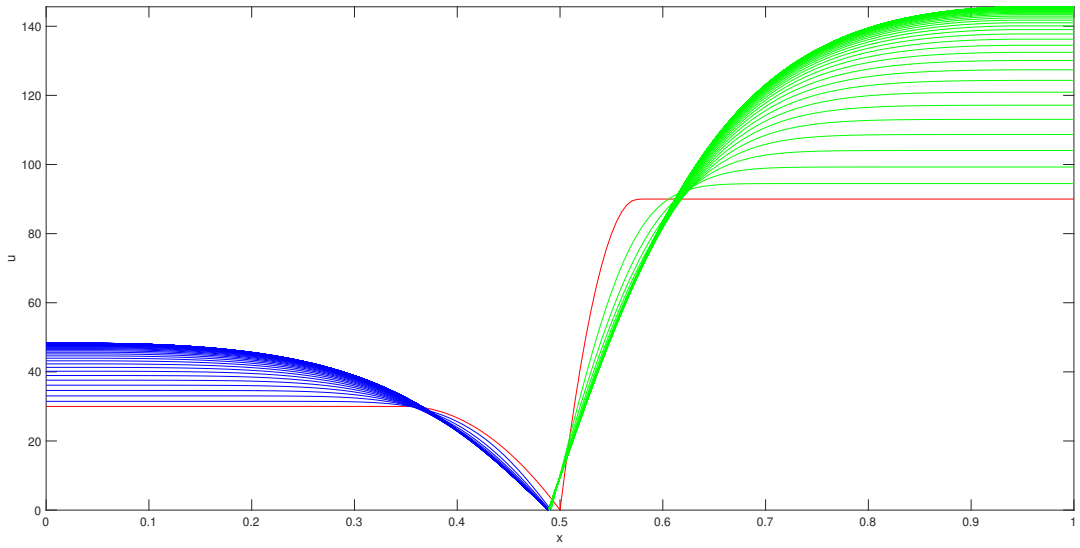

Figure 6. Result of competition model at $t = 9$, considering the effect of altered carrying capacities. Here we use $\delta_1 = \delta_2 = 0.01$, $k_1 = 50, k_2 = 150$, $r_1 = r_2 = 1$ and $\mu = 3$. We run the model with a time step of 0.00001 for 150,000 iterations and plot the results every 0.01. The figure shows the rapid territorial gains. The initial conditions are shown in red, with species 1 in blue and species 2 in green.

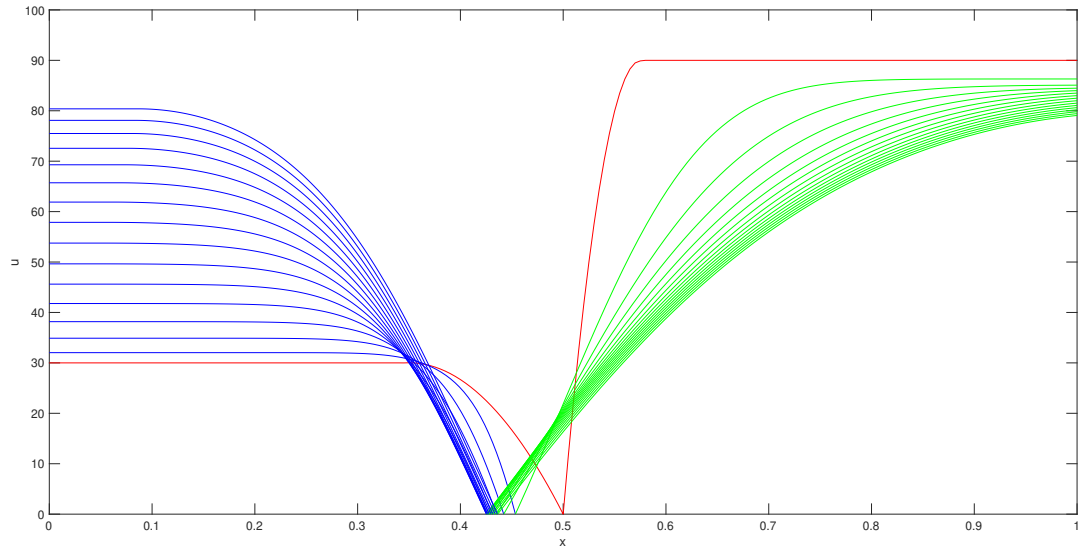

Figure 7. Result of competition model at $t = 1.5$, considering the effect of an increased diffusion rate for species 2. Here we use $\delta_1 = 0.01, \delta_2 = 0.05$, $k_1 = k_2 = 100$, $r_1 = r_2 = 1$ and $\mu = 3$. We run the model with a time step of 0.00001 for 150,000 iterations and plot the results every 0.01. The figure shows the rapid territorial gains of species 2 over species 1 due to its high diffusion rate. The initial conditions are shown in red, with species 1 in blue and species 2 in green.

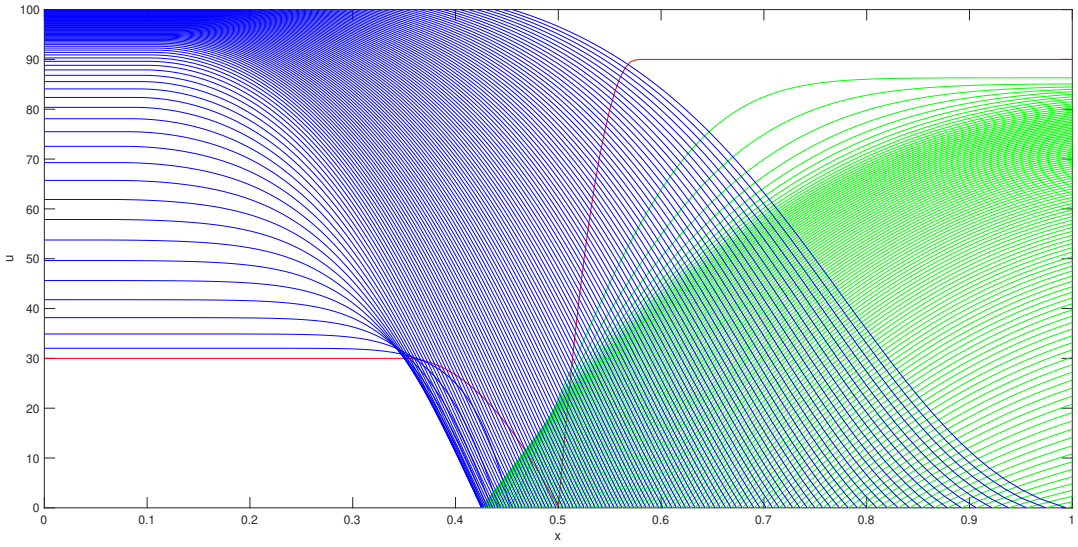

Figure 8. Result of competition model at $t = 11$, considering the effect of an increased diffusion rate for species 2. Here we use $\delta_1 = 0.01, \delta_2 = 0.05$, $k_1 = k_2 = 100$, $r_1 = r_2 = 1$ and $\mu = 3$. We run the model with a time step of 0.00001 for 1,100,000 iterations and plot the results every 0.01. We see that the initial diffusion-driven gains by species 2 are reversed, and that the overall growth characteristics are dominating so that species 1 is gaining territory. The initial conditions are shown in red, with species 1 in blue and species 2 in green.

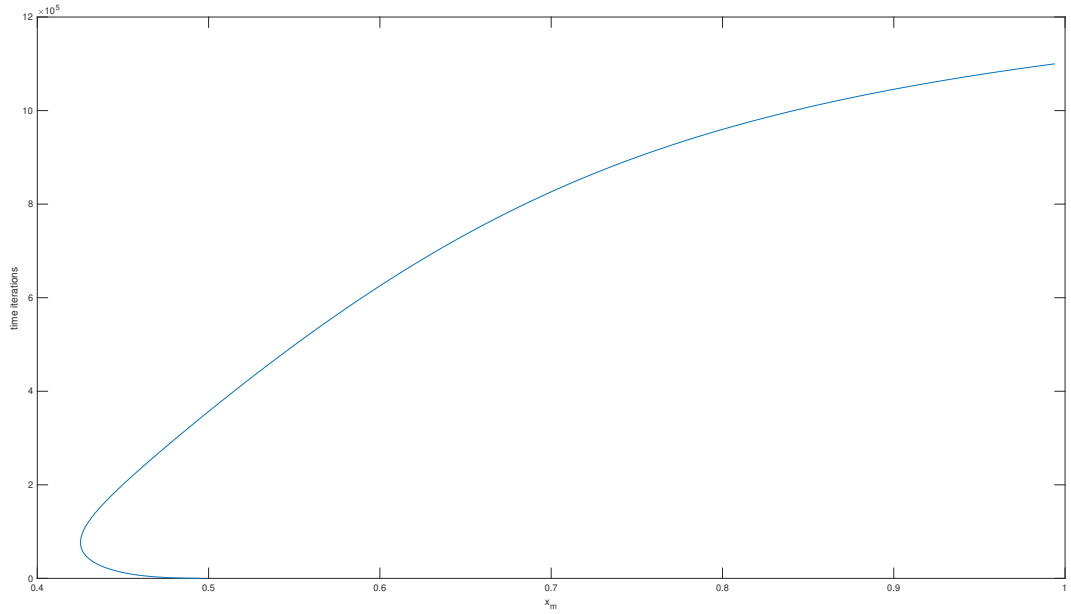

Figure 9. Position of interface, x_m, showing interface movement for the competition model at up to $t = 11$, considering the effect of an increased diffusion rate for species 2. Here we use $\delta_1 = 0.01, \delta_2 = 0.05$, $k_1 = k_2 = 100$, $r_1 = r_2 = 1$ and $\mu = 3$. We run the model with a time step of 0.00001 for 1,100,000 iterations. Due to the growth characteristics we can see interesting temporal effects. Here the interface velocity has actually reversed direction as the system changes from diffusion-dominated to growth-dominated.

4. Discussion

In this paper we constructed a moving mesh finite difference method based on conservation for the Lotka-Volterra competition system with a high competition limit, such that the species are completely spatially segregated at an interface. The system of equations produced interesting and realistic behaviour in a very stable model. We were able to implement the model with a wide variety of creative parameter combinations, and observed various effects dominating in turn as the populations evolve through time.

The illustrations presented above give confidence that the model and the moving mesh finite difference approach is likely to be able to satisfy the requirements of modelling a wide variety of competition systems and is numerically stable to a large choice of set-up parameters and is able to produce complex behaviours without problems.

For a set of parameters that favour species 1 we see an increasing interface velocity in the initial stages followed by a change in direction and a long steady phase where the interface velocity is approximately constant. Although the population of species 2 initially makes territorial gains it is eventually wiped out by the competition with species 1. As the annihilation of species 2 is approached, the interface velocity increases again. This is due to the low population of species 2 affecting its ability to compete with species 1.

If the growth of species 1 is restricted by lowering its carrying capacity, interestingly, we observe that neither species is dominant, even though all the competition and diffusion characteristics are unchanged. Therefore, density dependence can affect the competitive ability of a species.

In the case of increasing the diffusion rate for species 2, this species is able to make initial territorial gains, even though the competition rate is unaltered. However, as time goes on, growth and competition characteristics become increasingly important and species 1 becomes more dominant, so the interface velocity reverses direction.

A natural extension is to two dimensions along the lines described in [18], a first attempt appearing in reference [25] which foundered only on stability issues. In further work it would be interesting to compare the behaviour of the model against an empirical data set. The model lends itself to alterations to the logistic terms and changes to parameters without the need for any further development. The aim should be to understand the requirements from both a mathematical and quantitative perspective.

Author Contributions: Both authors made equal contributions to this paper. Both authors have read and agreed to the published version of the manuscript.

Funding: This work was supported by the UK Natural Environment Research Council [grant number NE/P012345/1].

Institutional Review Board Statement: Not applicable.

Informed Consent Statement: Not applicable.

Data Availability Statement: Not applicable.

Acknowledgments: The authors wish to acknowledge the work of Watkins [7,25] using finite elements in the motivation for this work.

Conflicts of Interest: The authors declare no conflict of interest.

Abbreviations

The following abbreviations are used in this manuscript:

MMFDM	Moving Mesh Finite Difference Method
MMPDE	Moving Mesh Partial Differential Equations
PDE	Partial Differential Equations

References

1. Guo, J.S.; Wu, C.H. Dynamics for a two-species competition–diffusion model with two free boundaries. *Nonlinearity* **2015**, *28*, 1–27. [CrossRef]
2. Guo, J.S.; Wu, C.H. On a Free Boundary Problem for a Two-Species Weak Competition System. *J. Dyn. Differ. Equ.* **2012**, *24*, 873–895. [CrossRef]
3. Wu, C.H. The minimal habitat size for spreading in a weak competition system with two free boundaries. *J. Differ. Equ.* **2015**, *259*, 873–897. [CrossRef]
4. Wang, M.; Zhao, J. Free Boundary Problems for a Lotka–Volterra Competition System. *J. Dyn. Diff. Equ.* **2014**, *26*, 655–672. [CrossRef]
5. Gardner, R.A. Existence and stability of travelling wave solutions of competition models: A degree theoretic approach. *J. Differ. Equ.* **1982**, *44*, 343–364. [CrossRef]
6. Liu, S.; Liu, X. Numerical Methods for a Two-Species Competition-Diffusion Model with Free Boundaries. *Mathematics* **2018**, *6*, 72. [CrossRef]
7. Watkins, A.R.; Baines, M.J. *A Two-Phase Moving Mesh Finite Element Model of Segregated Competition-Diffusion Preprint MPCS-2018-07*; Department of Mathematics and Statistics, University of Reading: Reading, UK, 2017.
8. Budd, C.J.; Huang, W.; Russell, R.D. Adaptivity with moving grids. *Acta Numer.* **2009**, *18*, 111–241. [CrossRef]
9. Beckett, G.; Mackenzie, J.A.; Robertson, M.L. A moving mesh finite element method for the solution of two-dimensional Stefan problems. *J. Comput. Phys.* **2001**, *168*, 500–518.
10. Huang, W.; Ren, Y.; Russell, R.D. Moving mesh partial differential equations (MMPDEs) based on the equidistribution principle. *SIAM J. Sci. Comput.* **1994**, *31*, 709–730. [CrossRef]
11. Miller, K.; Miller, R.N. Moving finite elements. I. *SIAM J. Numer. Anal.* **1981**, *18*, 1019–1032. [CrossRef]
12. Miller, K. Moving finite elements. II. *SIAM J. Numer. Anal.* **1981**, *18*, 1033–1057. [CrossRef]
13. Baines, M.J.; Hubbard, M.E.; Jimack, P.K. A moving mesh finite element algorithm for the adaptive solution of time-dependent partial differential equations with moving boundaries. *Appl. Numer. Math.* **2005**, *54*, 450–469. [CrossRef]
14. Baines, M.J.; Hubbard, M.E.; Jimack, P.K. Velocity-based moving mesh methods for nonlinear partial differential equations. *Commun. Comput. Phys.* **2011**, *10*, 509–576. [CrossRef]
15. Lee, T.E.; Baines, M.J.; Langdon, S. A finite difference moving mesh method based on conservation for moving boundary problems. *J. Comp. Appl. Math.* **2015**, *288*, 1–17. [CrossRef]
16. Baines, M.J.; Hubbard, M.E.; Jimack, P.K.; Mahmood, R. A moving-mesh finite element method and its application to the numerical solution of phase-change problems. *Commun. Comput. Phys.* **2009**, *6*, 595–624. [CrossRef]
17. Hilhorst, D.; Mimura, M.; Schätzle, R. Vanishing latent heat limit in a Stefan-like problem arising in biology. *Nonlinear Anal. Real World Appl.* **2003**, *4*, 261–285.
18. Harker, A.H. The classical Stefan problem: Basic concepts, modelling and analysis with quasi-analytical solutions and methods. *Contemp. Phys.* **2018**, *59*, 428–429. [CrossRef]
19. Crooks, E.C.; Dancer, E.N.; Hilhorst, D.; Mimura, M.; Ninomiya, H. Spatial segregation limit of a competition-diffusion system with Dirichlet boundary conditions. *Nonlinear Anal. Real World Appl.* **2004**, *5*, 645–665. [CrossRef]
20. Dancer, E.N.; Hilhorst, D.; Mimura, M.; Peletier, L.A. Spatial segregation limit of a competition-diffusion system. *Eur. J. Appl. Math.* **1999**, *10*, 97–115. [CrossRef]
21. Hilhorst, D.; Iida, M.; Mimura, M.; Ninomiya, H. A competition–diffusion system approximation to the classical two-phase Stefan problem. *Japan J. Indust. Appl. Math.* **2001**, *18*, 161–180. [CrossRef]
22. Hardin, G. The Competitive Exclusion Principle. *Science* **1960**, *131*, 1292–1297. [CrossRef] [PubMed]
23. Main, B.E. Solving Richards' Equation Using Fixed and Moving Mesh Schemes. Master's Thesis, Department of Mathematics, University of Reading, Reading, UK, 2011.
24. Baines, M.J. Explicit time stepping for moving meshes. *J. Math. Study* **2015**, *48*, 93–105. [CrossRef]
25. Watkins, A.R. A Moving Mesh Finite Element Method and Its Application to Population Dynamics. Ph.D. Thesis, University of Reading, Reading, UK, 2017.